

A HYCOM modeling study of the Persian Gulf:

1. Model configurations and surface circulation

Fengchao Yao¹ and William E. Johns¹

Received 8 September 2009; revised 8 August 2010; accepted 19 August 2010; published 19 November 2010.

[1] The circulation and water mass transformation processes in the Persian Gulf and the water exchange with the Indian Ocean through the Strait of Hormuz are studied using the Hybrid Coordinate Ocean Model (HYCOM). Model results show that the Indian Ocean Surface Water (IOSW) propagates in two branches into the gulf, one along the Iranian coast toward the northern gulf and the other one onto the southern banks driven by the Ekman drift due to the prevailing northwesterly winds. These two branches of inflow form two cyclonic gyres in the northern and in the southern gulf. A salinity front separates the fresher intruding IOSW from the saltier waters in the gulf. Eddies with size of about 100 km are fully developed along the salinity front in summer. The intrusion of the IOSW in the model extends much farther into the gulf in summer than in winter. By analyzing the salt balance in the basin and conducting sensitivity experiments, we show that it is the balance between the advection of IOSW and vertical salt flux induced by mixing that mainly controls the seasonal variation of the surface salinity. Surface wind stress plays a secondary role in modulating the seasonal intrusion of the IOSW. High-frequency atmospheric forcing produces more realistic surface temperatures than obtained from climatological forcing, as a result of increased heat loss in winter. However, the high-frequency forcing does not change significantly the general features of the circulation.

Citation: Yao, F., and W. E. Johns (2010), A HYCOM modeling study of the Persian Gulf: 1. Model configurations and surface circulation, *J. Geophys. Res.*, 115, C11017, doi:10.1029/2009JC005781.

1. Introduction

[2] The Persian Gulf, also known as the Arabian Gulf (hereinafter referred as the gulf), lies between the Arabian Peninsula and southwestern Iran, connected with the Gulf of Oman and the Indian Ocean through the Strait of Hormuz (hereinafter referred as the strait) (Figure 1). The gulf is a shallow, semienclosed marginal sea resulting from continuous deposition in a once deep basin [Emery, 1956]. The length of the gulf is about 1000 km in NW-SE direction, the width varies from a maximum of 338 km to a minimum of 56 km in the strait, and the surface area is approximately 3.3×10^5 km². The bathymetry of the gulf is asymmetric: a trough through the strait extends northwest along the Iranian coast; a shallow bank area with depths less than 20 m exists in the southwestern gulf. With an average depth of 35 m and a maximum depth of 110 m in the strait, the bottom of the gulf drops quickly, without significant sills in the strait, to more than 2000 m within 200 km into the Gulf of Oman.

[3] The Persian Gulf Water (PGW), one of the most saline water masses in the world ocean, is formed in the gulf due to excessive net fresh water loss to the atmosphere and con-

stricted water exchange with the open ocean through the strait. The dense PGW exits the gulf as a deep outflow and induces an inverse estuarine type water exchange through the strait. Basically, the gulf is similar to other land-locked marginal seas, such as the Red Sea and Mediterranean Sea. However, the circulation in the gulf possesses its own uniqueness due to the much shallower depths of the basin, wider strait to the open ocean and lack of a distinct sill, and, compared to the Mediterranean Sea and the Red Sea, the physical oceanography in the gulf has been less extensively studied.

[4] Observations of the water properties and circulation in the gulf are limited in temporal and spatial coverage. There are only a few published basin-wide survey results: Emery [1956] on a 1948 summer cruise by the German ship *Meteor*; Brewer and Dyrssen [1985] on the 1976 wintertime expedition of the *Atlantis* from Woods Hole Oceanographic Institution, and Reynolds [1993] on surveys in February and June 1992 on the *Mt. Mitchell* expedition. Swift and Bower [2003] compiled the available hydrographic data (with some overlap with the aforementioned surveys) to describe the aspects of the seasonal variability (from January to August) of the water properties in the gulf. Johns *et al.* [2003] conducted measurements of the water exchange in the strait, consisting of a mooring site in the deep channel in the strait and four seasonal transects across the strait. These measurements, for the first time, provided a long-term observation of the exchange process in the strait and are the direct motivation for this study.

¹Division of Meteorology and Physical Oceanography, Rosenstiel School of Marine and Atmospheric Science, University of Miami, Miami, Florida, USA.

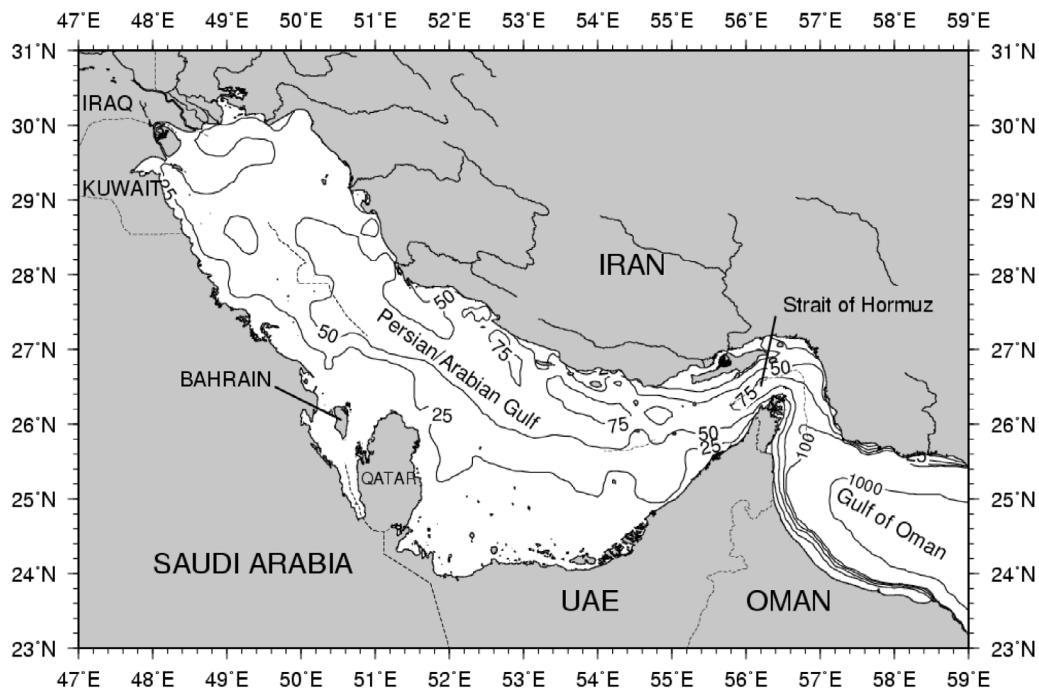


Figure 1. Map of the gulf region. Water depths in m are derived from the 2 min ETOPO2 database.

[5] The physical processes controlling the circulation and the water mass properties in the gulf are complicated and dynamical factors acting on different temporal and spatial scales are involved. The available observations are not seasonally complete enough to give a description of the annual cycle of the circulation, and numerical modeling studies are sparse as well. The model study by *Chao et al.* [1992] focused on the sensitivity of the surface circulation to various forcing mechanisms, including river discharge, heat flux, fresh water flux and surface wind stress. *Chao et al.* [1992] identified the fresh water flux and wind stress as the essential forcing to reproduce the observed circulation, but the processes of water mass formation were not discussed. *Kämpf and Sadrinasab's* [2006] numerical study suggests the surface circulation the gulf experiences a distinct seasonal cycle, but controlling forcing mechanisms are not further investigated. A recent numerical study by [*Thoppil and Hogan, 2009*] explored mechanisms of the short-term (several days to a few weeks) variability of the dense outflow in the strait and found that the observed episodic salinity outflow events are the result of mesoscale cyclones induced by fluctuations in the wind stress forcing. Still, many basic questions regarding the circulation in the gulf remain unanswered, such as the dense water formation processes, the general circulation pattern and its seasonal variability, and the respective roles played by the wind stress and buoyancy flux. With greatly improved computing power and more sophisticated Ocean General Circulation Models, high-resolution numerical simulations provide a viable way to explore these questions. In this study, we use the Hybrid Coordinate Ocean Model (HYCOM) to examine the seasonal circulation pattern and water mass formation processes in the gulf and the roles played by different atmospheric forcing mechanisms.

[6] This study is presented in two papers. This paper is focused on the model configurations and surface circulation derived from the model and is organized as follows. Observational background of the surface circulation in the gulf is presented in section 2. In section 3, the configurations of the simulations, including the model domain, initialization, vertical discretization and experiment setups, are provided in detail. In section 4, the characteristics of the surface forcing are discussed. Section 5 describes the seasonal surface circulation arising from numerical simulations with different atmospheric forcing. In section 6, the mechanisms controlling the seasonal surface salinity front are investigated by diagnosing the model results. A short summary is given in section 7. Numerical results of the water mass formation and export processes are presented by *Yao and Johns* [2010].

2. Background

[7] The surface circulation in the gulf as summarized by *Reynolds* [1993] is given in Figure 2, and the surface hydrographic fields from *Reynolds' [1993]* winter and early summer survey are reproduced in Figures 3a and 3b, respectively. The annual mean Indian Ocean Surface Water (IOSW) entering the gulf through the northern part of the strait is deflected along the Iranian coast and appears to form a basin-wide cyclonic circulation in the southern gulf (Figure 2). In the northern gulf, there are two downwind coastal currents on both the Arabian and Iranian coasts.

[8] Surface salinity fields (Figures 3a and 3b) indicate that the relatively low-salinity IOSW undergoes a salinity increase and is transformed into high-salinity waters (>40 practical salinity unit (psu)) in the northern gulf and in the shallow southern gulf in both winter and early summer. In the shallow

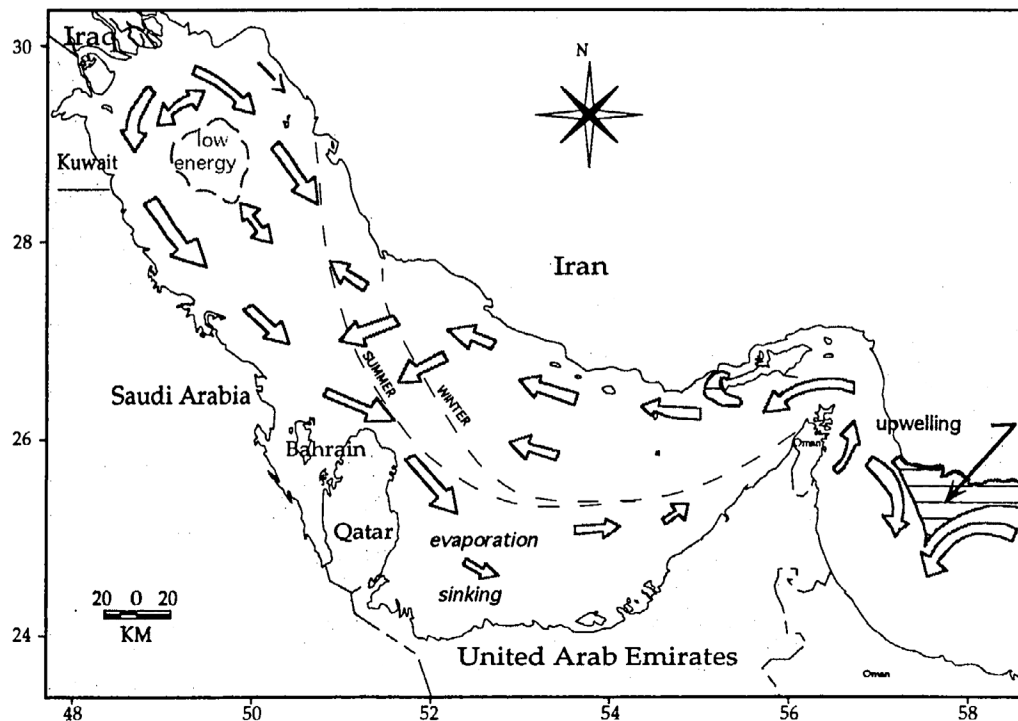


Figure 2. Schematic of the surface circulation in the gulf summarized by Reynolds [1993]. The dashed lines in the central part of the gulf indicate the approximate seasonal location of the salinity front between the inflowing fresh IOSW and the more saline waters of the gulf.

coastal area along UAE and west of Qatar extremely high-salinity values (>50 psu) have been recorded by other observations [e.g., John *et al.*, 1990; Chandy *et al.*, 1990]. Both the surface temperature and salinity fields show pronounced seasonal variability, and as a combined result of low temperature and high-salinity, dense waters ($\sigma_\theta > 29.5$) are formed in the northern gulf and the southern banks. Interestingly, the salinity front separating the intruding IOSW and PGW extends much farther into the gulf in early summer than in winter; surface water with salinity less than 37 psu can reach up to 53°E in early summer, while it retreats to the strait (56°E) in winter. Such seasonal differences of the distributions of surface salinity also exist between the summer survey by Emery [1956] and the winter survey by Brewer and Dyrssen [1985]. The controlling mechanisms of this seasonal variation are studied in detail in section 6.

[9] On the synoptic scale, the gulf exhibits energetic features as shown by a snapshot image of surface temperature from Moderate-Resolution Imaging Spectroradiometer (MODIS) (Figure 4). There exists a meandering front between the warm Iranian coastal water and the cold water in the northwestern gulf. In the southern gulf, a pronounced cyclonic eddy can be seen entraining warm water from the southern banks. In general, little is known about the meso-scale variability in the gulf and it remains poorly studied.

3. Model Configurations

3.1. Overview of HYCOM

[10] HYCOM is a hydrostatic, primitive equation general circulation model that evolved from the Miami Isopycnal Coordinate Model (MICOM). Its general architecture and

initial validation is documented by Bleck [2002], followed by further developments by Halliwell [2004]. Flexible options for the vertical grid enable HYCOM to conserve water mass properties in the isopycnal coordinates when there is strong vertical stratification and provide adequate vertical resolution in regions with weak stratification, such as the surface mixed layer. In HYCOM, different schemes are incorporated for the vertical mixing, and the K Profile Parameterization (KPP) [Large *et al.*, 1994] is used in this study. The NASA Goddard Institute for Space Studies level 2 turbulence closure [Canuto *et al.*, 2001, 2002] is also tested in the study and gives similar results. This is among the first applications of the HYCOM in a shallow semienclosed marginal sea.

3.2. General Configurations

[11] The domain for the simulation includes the entire gulf and most of the Gulf of Oman, with the open boundary located in the eastern side of the Gulf of Oman. The grid points are projected onto a Mercator projection. The horizontal resolution is set to $1/20$ degree (~ 5 km), which is fine enough to resolve the strait and the Rossby radius of deformation (about 20 km) as well. Topography is interpolated from the 2 min ETOPO2 topographic data set, with corrections to some coastal areas according to ETOPO5 (Figure 5). The target densities for the layers in HYCOM range from sigma 23 to 29, with 13 equally distributed layers. The minimum layer depth is set to 3.0 m. The vertical coordinates are determined geometrically (i.e., z level or sigma coordinate) if there is not enough vertical stratification. A buffer zone is used at the eastern boundary in the Gulf of Oman where water properties are restored to seasonally observed values from the Levitus' climatology [Levitus *et al.*, 1994;

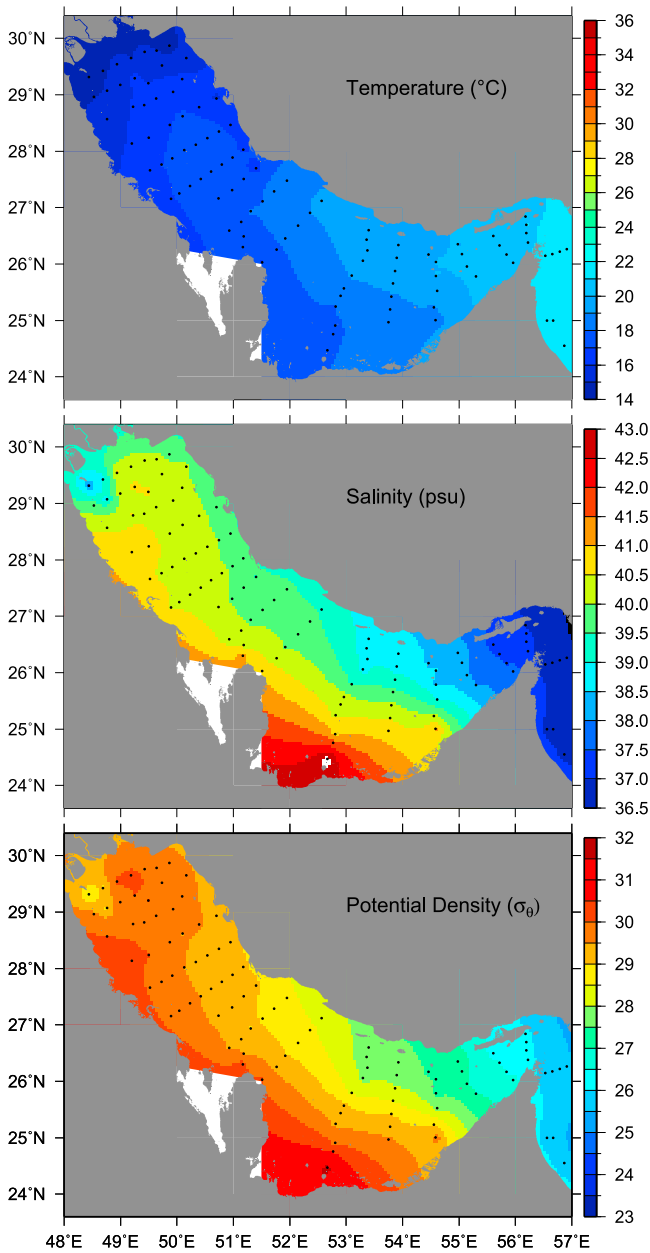


Figure 3a. Surface fields of temperature, salinity, and potential density during Reynolds' [1993] winter survey. The black dots represents the conductivity-temperature-depth (CTD) stations. Areas without enough coverage are left blank.

Levitus and Boyer, 1994]. The buffer zone has a width of about 40 km with a restoring time of 60 days. Tidal forcing has little effect on the residual circulation in the gulf and is not included in this study. The river discharges, mainly from the northern end of the gulf, only affect the local circulation [Chao et al., 1992] and are not included in the simulations.

3.3. Experiments With Different Atmospheric Forcing

[12] The circulation and water mass properties in the gulf are driven mainly by the surface fluxes including the momentum flux (wind stress), heat flux and fresh water flux.

The evaporation and the turbulent air-sea heat fluxes (sensible heat flux and latent heat flux) in HYCOM are parameterized from the basic meteorological variables using the bulk formula of Kara et al. [2000]. To investigate the role played by high-frequency variability in the atmospheric forcing, the basic meteorological variables in our study are derived from two sources: (1) the COADS (Comprehensive Ocean-Atmosphere Data Set [Woodruff et al., 1993]) monthly climatology and (2) high-frequency and high-resolution MM5 (the Fifth-Generation NCAR/Penn State Mesoscale Model [Dudhia, 1993]) output for the year of 2001. The COADS

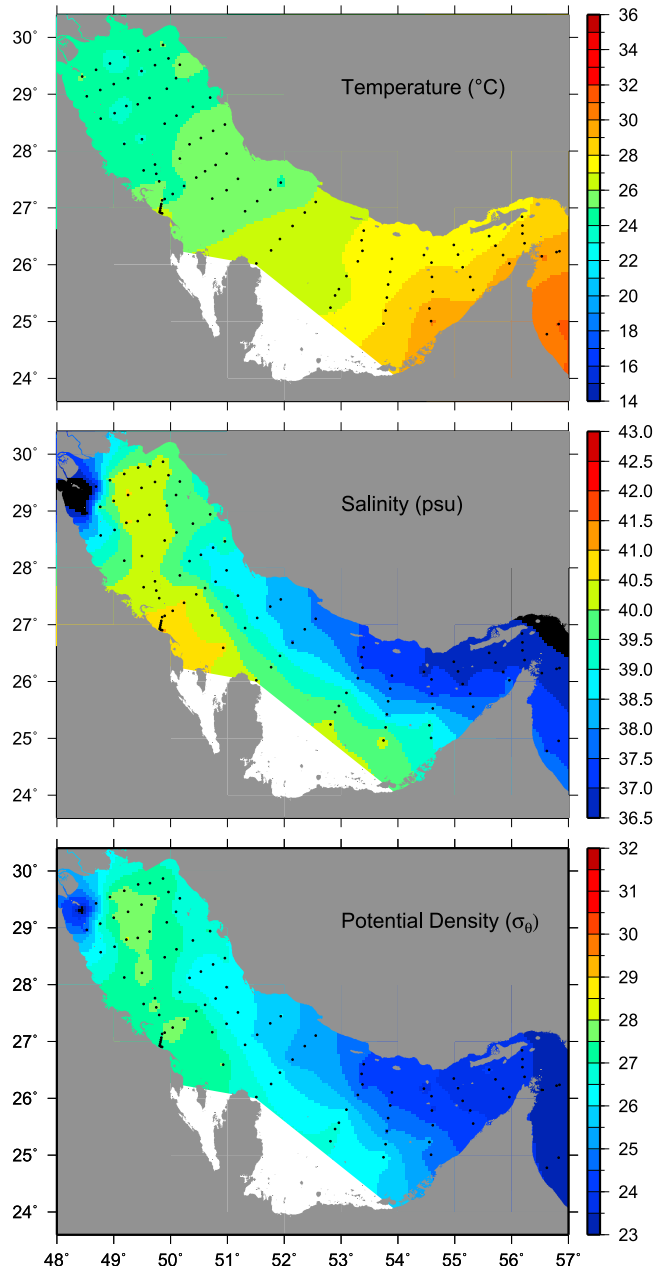


Figure 3b. Surface fields of temperature, salinity, and potential density during Reynolds' [1993] early summer survey.

MODIS SST Image on September 11, 2003

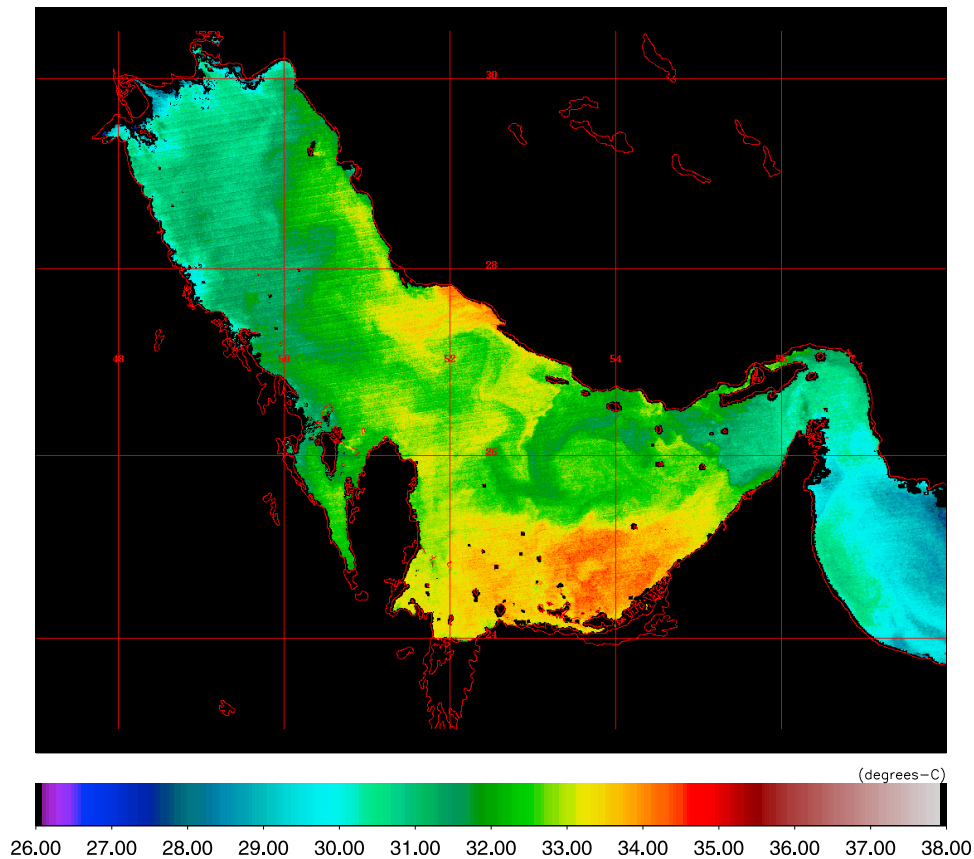


Figure 4. MODIS sea surface temperature image of the gulf on 11 September 2003. A notable synoptic feature is the eddy centered around 53.8°E, 22.9°N.

monthly climatology is based on archived ship observations with relatively low resolution (1×1 degree). The MM5 provides hourly surface meteorological variables with resolution of ~ 30 km and is capable of resolving the synoptic and diurnal variability missing in the COADS monthly climatology, as well as orographic effects.

[13] The radiative fluxes (short-wave and long-wave radiative heat flux) derived from COADS for the gulf region exhibit systematic biases as described by *Johns et al.* [2003], so they are corrected according to the values of *Johns et al.* [2003]. To clearly isolate the effect of high-frequency atmospheric forcing, the high-frequency surface meteorological variables used in the model are constructed from the COADS monthly meteorological field with only anomalies added from the MM5 output for the year of 2001, to ensure the same overall seasonal cycle of the atmosphere. The same correction to the radiative fluxes is also applied to the high-frequency forcing. The details of surface flux forcing are discussed in section 4.

[14] Three experiments with different atmospheric forcing are designed. The first run is forced with the COADS monthly meteorology with corrected radiative fluxes to investigate the seasonal patterns of the circulation. The second experiment is forced with only buoyancy flux from the COADS monthly meteorology. The surface wind stress in this experiment is set to zero, but the wind speed is used to parameterize the heat

and fresh water fluxes. This experiment directly investigates the relative role played by the surface wind stress. Both experiments are run for 10 years, which is sufficient for an equilibrium circulation to be well established. In the third experiment, the first experiment, after the 10 year climatological run, is extended with the 1 year high-frequency forcing repeatedly for additional 4 years. This experiment is used to investigate the effect of the high-frequency variability on the water mass formation and circulation.

3.4. Initial Adjustment

[15] The model is initialized by the salinity and temperature fields interpolated from the Levitus' climatology [*Levitus et al.*, 1994; *Levitus and Boyer*, 1994] without motion. The residence time of the gulf is estimated to be 5 years and the overturning time scale to be 2–3 years [*Hunter*, 1982], so we can expect a relatively quick adjustment time for the gulf to reach equilibrium. As a proxy of the adjustment process, figure 6 shows the evolution of the gulf-wide averaged temperature and salinity for 10 years of the climatological run and subsequent 4 years of high-frequency run. In the climatological run the temperature reaches a seasonal equilibrium after 1 year and the salinity reaches equilibrium after 4 years. In the high-frequency run, the temperature adjusts to a lower temperature, and the salinity adjusts to a slightly higher value. The reasons will be discussed in detail later. The results from

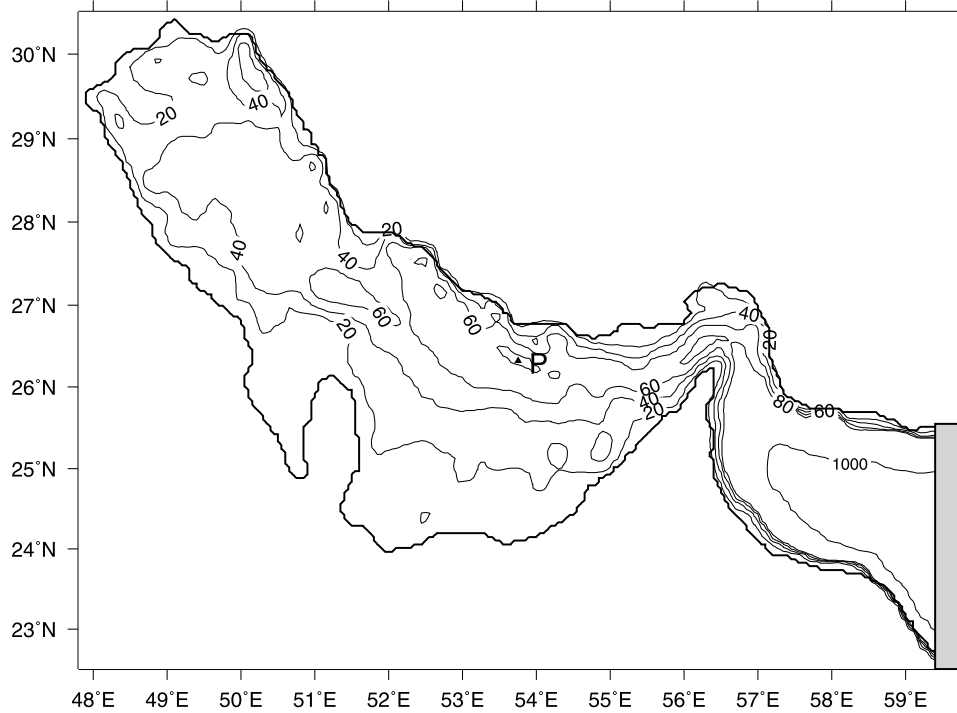


Figure 5. Model domain and topography derived from the ETOPO2 database for the HYCOM experiments. A buffer zone of ~40 km width (shaded area) is located along the eastern boundary in the Gulf of Oman. Point *P* is the location of the salt budget analysis in section 6.

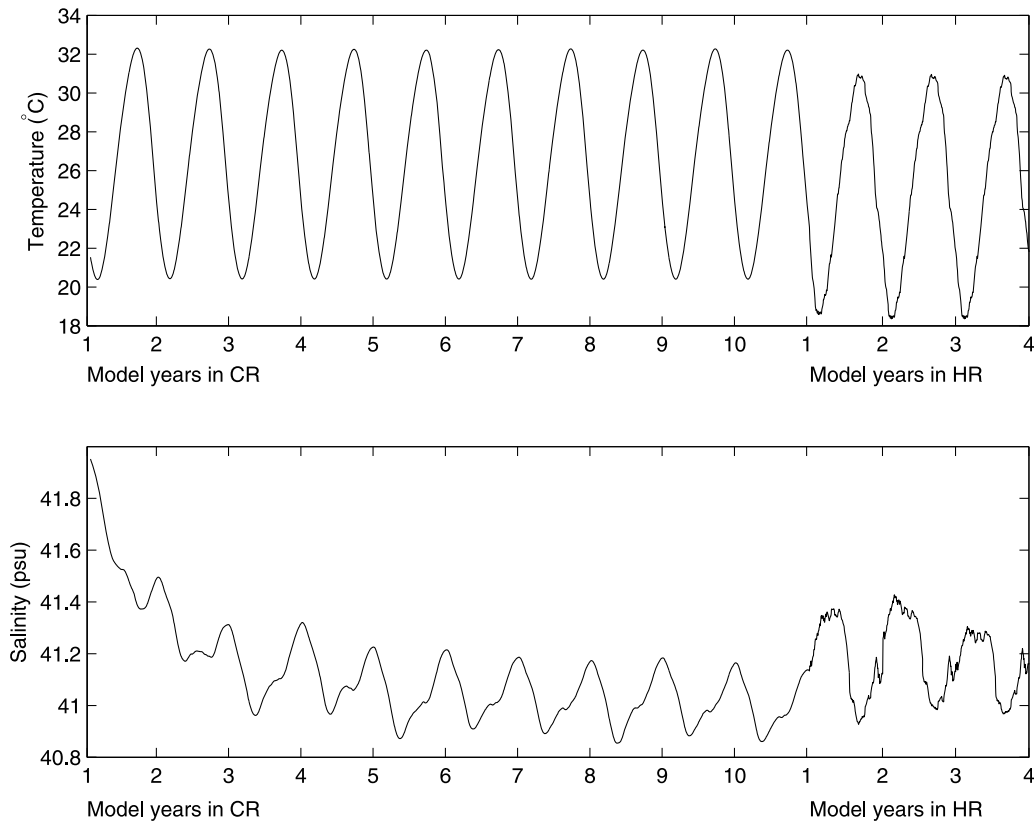


Figure 6. Adjustment of the basin-wide averaged (top) temperature and (bottom) salinity in the climatological run (CR) and the high-frequency run (HR).

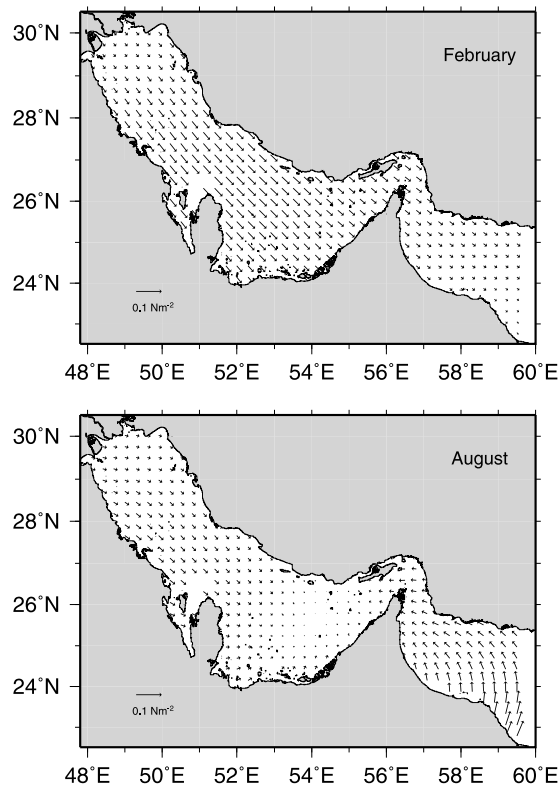


Figure 7. Surface wind stresses derived from the COADS monthly climatology for (top) February and (bottom) August in the gulf.

the 10th year of the climatological run are analyzed to represent the equilibrium state and seasonal cycle.

4. Surface Fluxes

[16] Surface wind stresses in summer and winter interpolated from the COADS monthly climatology are shown in Figure 7. The surface wind stress, steered by the surrounding mountains in the Iranian coast, is westerly or northwesterly throughout the year, i.e., along the axis of the gulf. The wind stress is, however, considerably stronger in winter than in summer. In contrast, the winds in the Gulf of Oman seasonally reverse with the Indian monsoon system, being northwesterly in the winter monsoon (October–May) and southeasterly in the summer monsoon (June–September).

[17] The high-frequency forcing resolves both the synoptic and diurnal variability. Time series of the high-frequency surface wind stress, surface air temperature, net heat flux and net freshwater flux for November at 49.75°E , 28.76°N in the central northern gulf are plotted in Figure 8. In winter and late fall, the atmospheric forcing is characterized by synoptic weather events associated with frontal passages. The synoptic weather systems cause strong northwesterly winds that last 3–5 days and air temperature drops of about $5\text{--}10^{\circ}\text{C}$. These events cause increased heat loss and spikes of water loss by evaporation. Time series of the sea surface temperature and ocean boundary layer depth in comparison to the climatological results are also shown to demonstrate the response of the gulf to the high-frequency forcing. The sea surface temperature is about $2\text{--}3^{\circ}\text{C}$ lower than that in climatological run.

The cooler sea surface temperature is the result of the cumulative effect of a series of extreme heat loss events. The boundary layer, which represents the depth where the vertical mixing can penetrate and is directly related to the surface forcing, exhibits strong fluctuations in the high-frequency run in response to the extremes of the high-frequency forcing, superimposed on a strong diurnal cycle.

[18] The basin averaged monthly mean values of the heat flux and fresh water flux from the climatological and high-frequency run are shown in Figure 9. The heat flux in the high-frequency run has the same seasonal pattern as in the climatological run, with maximum heat gain in May and maximum heat loss in November. The heat loss in November, December, and January are higher, mainly due to the higher latent heat loss by stronger evaporation in these months. The annual mean heat fluxes from the climatological and high-frequency run are -6.99 W/m^2 and -10.3 W/m^2 , respectively, and both are very close to *Johns et al.*'s [2003] estimated value of $-7 \pm 4\text{ W/m}^2$ (negative values mean heat loss from the ocean to the atmosphere). The net fresh water flux also exhibits a similar seasonal pattern. However, the fresh water loss in the high-frequency run is significantly higher in winter. This results in a larger annual mean fresh water loss of 1.43 m/yr compared with the climatological run (1.2 m/yr) and is now within the error bar of the estimate of $1.68 \pm 0.39\text{ m/yr}$ by *Johns et al.* [2003]. These higher values of the heat loss and fresh water flux can be attributed to the fact that the covariance of the wind speed, air temperature, and humidity are resolved in the high-frequency surface fields, particularly in the wintertime synoptic weather events. In the bulk formula, the turbulent heat fluxes are products of wind speed, air sea temperature difference and humidity difference. These variables have same mean values as in the climatological data, but their covariance on the short time scale can contribute the mean value of the heat fluxes.

5. Surface Circulation

5.1. Climatologically Forced Simulation

[19] The horizontal current fields are strongly coupled with the hydrographic fields, especially the salinity fields. The surface current fields superimposed on the salinity fields from the 10th year of climatological run are plotted in Figure 10. The results are averaged into four seasons, i.e., winter (January–March), spring (April–June), summer (July–September) and fall (October–December) in the surface 10 meters.

[20] The surface fields clearly show the seasonal variation of the intruding Indian Ocean Surface Water (IOSW) and its transformation into higher-salinity waters. Despite the distinct seasonal variability of the surface circulation, the general circulation pattern common to all seasons can be identified as follows. After entering the gulf through the strait, the low-salinity IOSW spreads into the interior of the basin generally in two pathways: one branch (northern branch) propagates along the Iranian coast and in summer can reach the basin west of Qatar to form a cyclonic circulation there. It drives a returning coastal current along the Arabian coast north of Qatar. The other branch (southern branch) veers southward to cross the basin to reach the southern UAE coast and also forms an overall cyclonic circulation in the southern gulf, which is in agreement with the summary by *Reynolds* [1993].

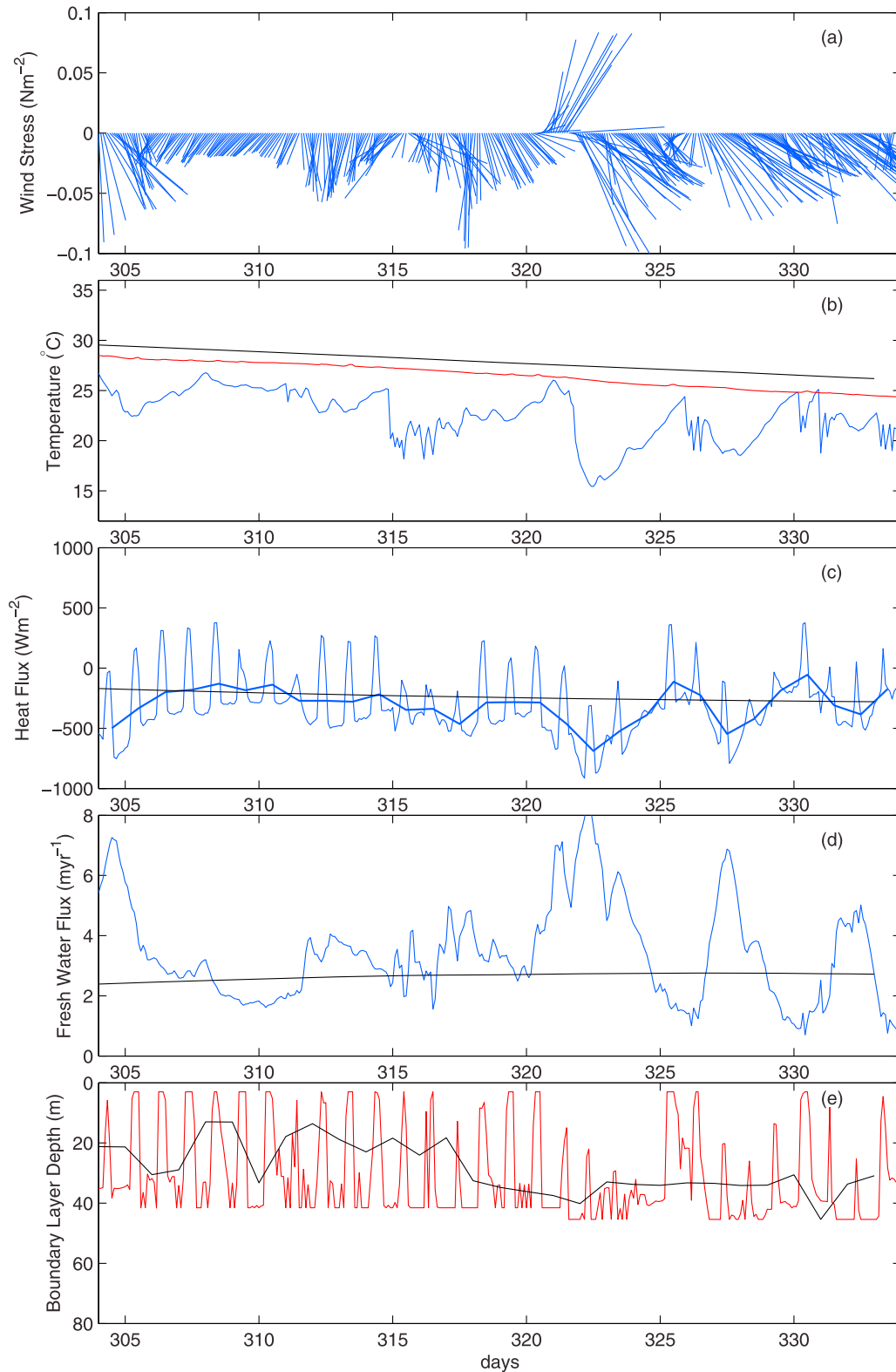


Figure 8. Time series of the high-frequency surface fluxes in the northern gulf for November 2001: (a) surface wind stresses, (b) surface air temperature (blue) and sea surface temperature (SST) from the high-frequency run (red) and SST from the climatological run (black), (c) high-frequency two hourly (thin blue) and daily mean (thick blue) net heat flux and climatological net heat flux (black), (d) high-frequency (blue) and climatological (black) fresh water flux, and (e) ocean boundary layer depths for high-frequency run (red) and for climatological run (black).

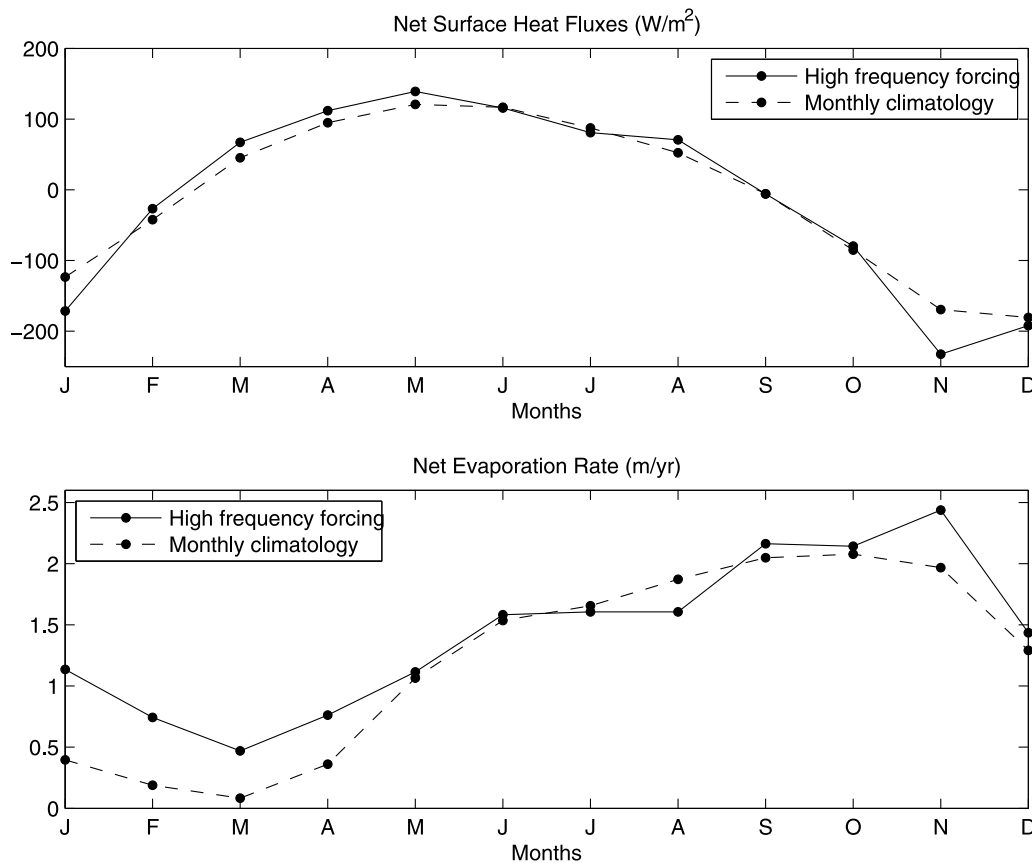


Figure 9. Monthly mean surface fluxes averaged over the gulf.

As will be seen in the buoyancy-only forcing experiment, this branch of flow is associated with the Ekman drift driven by the prevailing northwesterly winds. This general circulation pattern persists throughout the year, but it exhibits strong seasonal variation and is distorted by transient, synoptic features. In winter, opposed by stronger winds, the northern branch inflow does not penetrate past 27°N. As the winds relax in spring and summer and the seasonal thermocline is established, the current is coastally intensified and can reach nearly to the northern end of the gulf, bringing a tongue of low-salinity water up to 28°N. The southern branch is strongest in winter, partially driven by the stronger winds and partially by the sinking of the dense water in the southern gulf. As both branches of inflow spread into the gulf, the IOSW undergoes a considerable salinity increase by evaporation and mixing with ambient saltier water. Consistent with *Reynolds*' [1993] observation (Figure 3a), two isolated salinity maxima are found, one in the northern gulf and one in the southern gulf along the UAE coast, both with salinity >41 psu. The coastal flow along the Iranian coast in the northern gulf is driven by the surface wind stress and advects a higher-salinity water tongue along the coast in summer and fall.

[21] The salinity front that separates the low-salinity IOSW and hypersaline waters in the gulf moves farther into the gulf in summer than in winter, which is consistent with the observational results. The seasonal movement of the salinity front is accompanied by the development of energetic eddies. In spring the inflow develops unstable meanders along the salinity front. Fully developed eddies are formed in the

summer months. The eddies have a typical size of ~100 km. Considering the local baroclinic Rossby deformation Radius $R = (g'h)^{1/2}/f$, substitution of g' with 0.06 m/s^2 , $h = 60 \text{ m}$ and $F = 0.63 \times 10^{-4}$, the resulting R is ~30 km. Therefore the scale of the eddies is consistent with a baroclinic instability process occurring along the front. However, further energetics analysis, including mean potential and kinetic energy conversion rate, is needed to quantify and identify the nature of the instability. There is considerable spatial and temporal change in the Rossby deformation radius due to the change of the stratification. With about 1 unit difference in vertical density, the Rossby deformation radius in winter is about 7 km in the entire gulf, which is much smaller than that of about 30 km in summer along the salinity front. It will be seen later in the vertical sections covered by *Yao and Johns* [2010], the development of eddies is coincident with the establishment of the seasonal thermocline. The eddies propagate westward and coalesce into larger eddies probably due to an inverse energy cascade, until they are dissipated as the cooling in fall causes the thermocline to collapse. The existence of eddies with similar size is confirmed in the satellite image of the surface temperature (Figure 4). The eddies may play an important role in horizontally mixing waters across the salinity front.

5.2. Forcing Sensitivity Studies

[22] The seasonal surface current superimposed on salinity fields from the buoyancy-only forcing experiment are given in Figure 11 (compare with Figure 10). Several differences are notable. First is the lack of a current across the gulf to

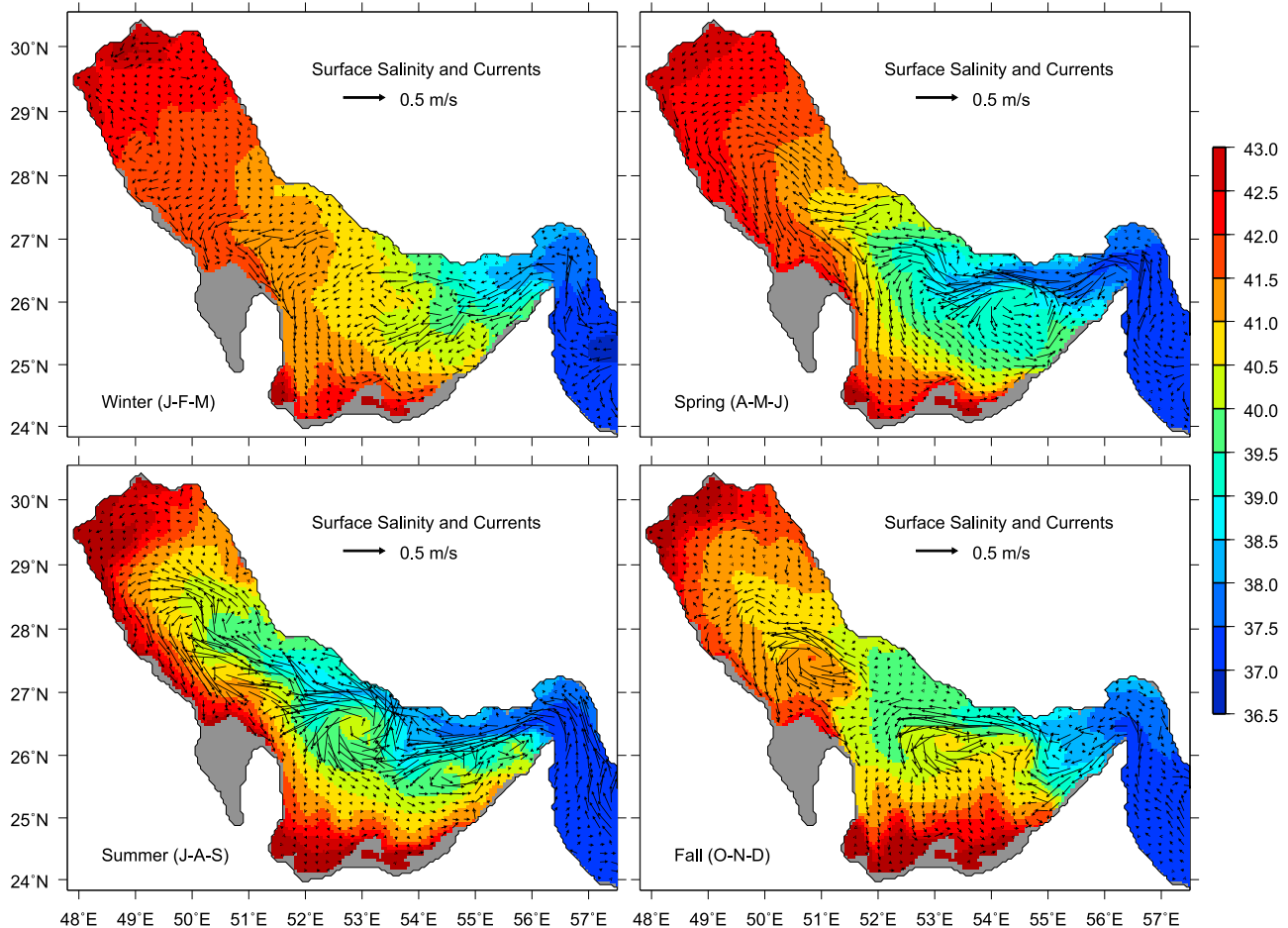


Figure 10. Seasonally averaged surface salinity fields and currents from the 10th year model output in the climatological run.

the southern banks, and an absence of cyclonic circulation patterns in the southern gulf. Second, the intruding IOSW extends markedly farther in the northern gulf, particularly in spring when it forms a cyclonic circulation up to the head of the gulf. The salinities in the northern gulf are consequently lower in all seasons. Conversely, the salinity on the shallow, coastal portion of the southern banks is higher due to the absence of southward Ekman transport of IOSW.

[23] The role of the surface wind stress on the circulation suggested in this experiment agrees with the theoretical model by *Csanady* [1982] about the wind driven circulation in a closed basin. The northwesterly winds in the northern gulf interior would produce Ekman flows to the right of the winds, and, in the absence of any other forcing, induce an upwind coastal current at the left coast (Arabian coast) and a downwind coastal current at the right coast (Iranian coast), thus forming an anticyclonic circulation in the northern basin. This anticyclonic circulation competes with the cyclonic thermohaline circulation, blocks the intruding inflow, and steers a portion of the inflow to form a cyclonic circulation the southern gulf.

[24] The seasonal mean surface circulation from the high-frequency forcing run does not deviate much from that in the climatological run and retains the main features of the circulation (Figure 12). The inflow from the strait spreads into the northern and southern gulf and forms two separate salty

water sources. The frontal eddies develop and dissipate in similar pattern to that in the climatological run. However, the winter inflow in the southern gulf is weaker as it is shifted to the southern banks. As in the time series in the northern gulf (Figure 8), the surface temperature is about 3°C colder across the gulf in both winter and summer, which is in much better agreement with observations in the gulf by *Reynolds* [1993] (compare to Figure 3a).

6. Seasonal Intrusion of the IOSW

[25] From both the observational [*Reynolds*, 1993; *Emery*, 1956; *Brewer and Dyrssen*, 1985] and numerical results (Figure 10 [*Kämpf and Sadrinasab*, 2006]), the spreading of the IOSW shows pronounced seasonal variation, extending much farther northwestward and southward into the gulf in late spring and summer than in winter. While the circulation in the gulf is mainly driven by seasonally varying surface heat flux, fresh water flux and wind stress, it is not straightforward to identify the seasonal forcing and physical processes responsible for the seasonal variability of the surface salinity.

[26] This intriguing question has puzzled researchers for decades and several hypotheses have been proposed to link the seasonality of different forcing to that of the surface salinity. *Schott* [1908] attributed the variability to the seasonally changing river discharges. *Emery* [1956] attrib-

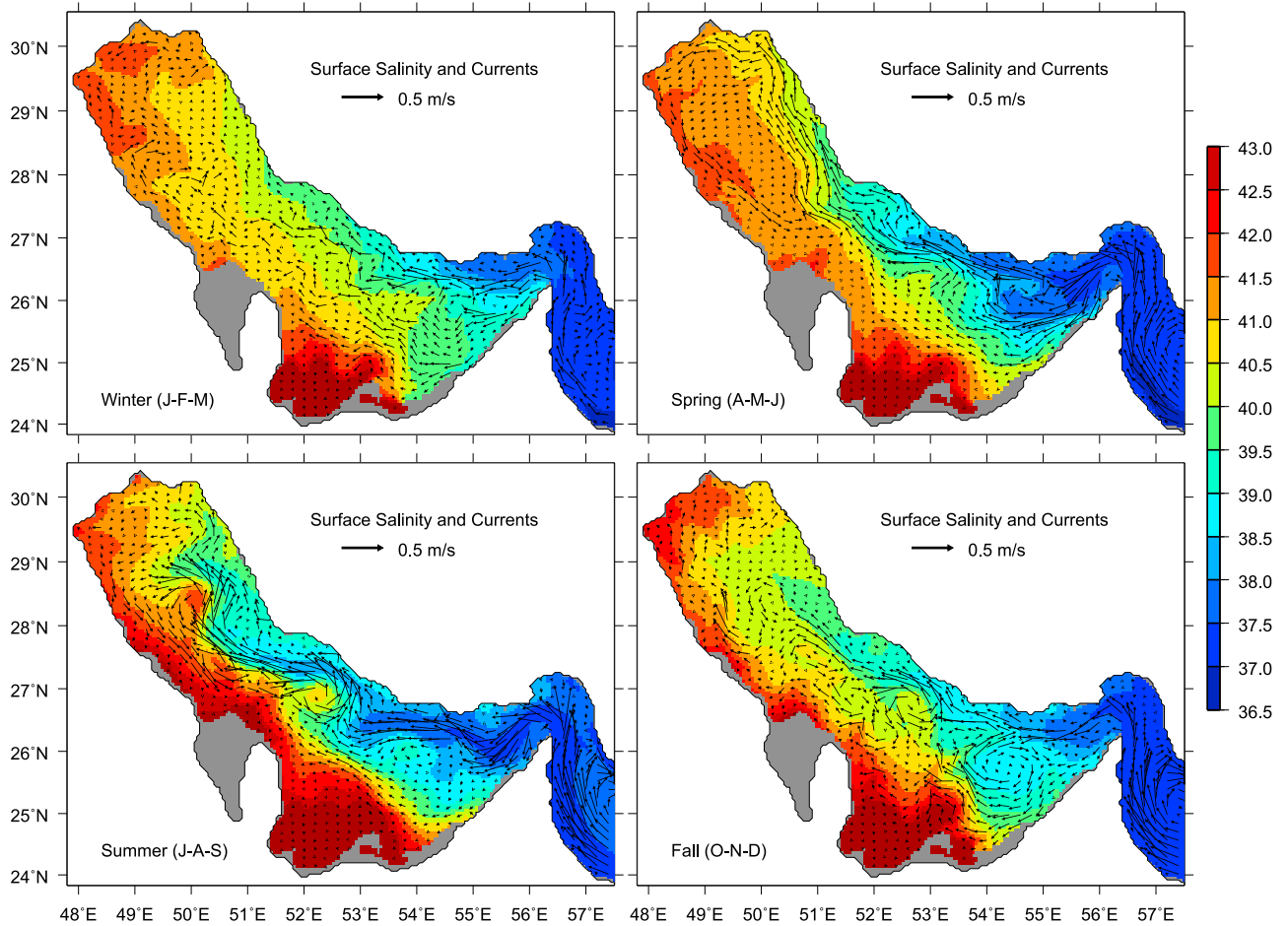


Figure 11. Seasonally averaged surface salinity fields and currents in the buoyancy-only forcing run.

uted the variability to a higher evaporation rate in winter over the gulf that would produce higher surface salinity. *Chao et al.* [1992] suggested the stronger winds in winter opposing the inflow would lead to the retreat of the low-salinity IOSW in winter. *Swift and Bower* [2003] argue that the seasonal variability is due to the evaporative lowering of sea surface height in the gulf during summer, which draws the IOSW farther into the gulf. Here, we will argue that a neglected process in the above hypotheses, i.e., the upward turbulent salt flux from the deep high-salinity waters to the surface waters, driven by the surface cooling and enhanced vertical mixing in winter, is actually the dominant factor in increasing the surface salinity in winter.

[27] The numerical simulation forced by the monthly climatology successfully captures the seasonal variability of the surface salinity and provides annual three-dimensional distribution of the salinity fields. The contribution to the change of the surface salinity by various dynamic and thermodynamic processes, including horizontal advection, horizontal diffusion, surface evaporation and vertical mixing, can be diagnosed directly from the model results.

[28] We begin by considering the salt balance at one fixed point, P , located at 53.75°E and 26.32°N (see Figure 5 for the location). This point experiences one of the highest-salinity variations in the gulf due to the seasonal advance and retreat of the IOSW intrusion. Time series of the vertical profiles of

salinity at point P are shown in Figure 13. Consistent with the passing of the salinity front, the salinity at P in the surface layer (<40 m) exhibits a distinct seasonal cycle. In winter (from January to March), P is occupied with high-salinity water (40.5–41 psu) with little vertical gradient. The low-salinity water with salinity less than 38.5 psu starts intruding from April and reaches a maximum depth of about 40 m in July. The upper layer salinity is increased to 40 psu from August to December.

[29] The salinity, S , in HYCOM is governed by the equation

$$\frac{\partial S}{\partial t} = -\left(u \frac{\partial S}{\partial x} + v \frac{\partial S}{\partial y}\right) + K_H \left(\frac{\partial^2 S}{\partial x^2} + \frac{\partial^2 S}{\partial y^2}\right) + \frac{\partial}{\partial z} \left(K_V \frac{\partial S}{\partial z}\right), \quad (1)$$

where u and v are horizontal velocities; K_H and K_V are the horizontal and vertical diffusivities, respectively. Consider the salt in a water column from the surface to a fixed depth h (here chosen to be 20 m). Integrating equation (1) vertically over this water column yields

$$\int_{-h}^0 \frac{\partial S}{\partial t} dz = - \int_{-h}^0 \left(u \frac{\partial S}{\partial x} + v \frac{\partial S}{\partial y}\right) dz + \int_{-h}^0 K_H \left(\frac{\partial^2 S}{\partial x^2} + \frac{\partial^2 S}{\partial y^2}\right) dz + F_b - F_s, \quad (2)$$

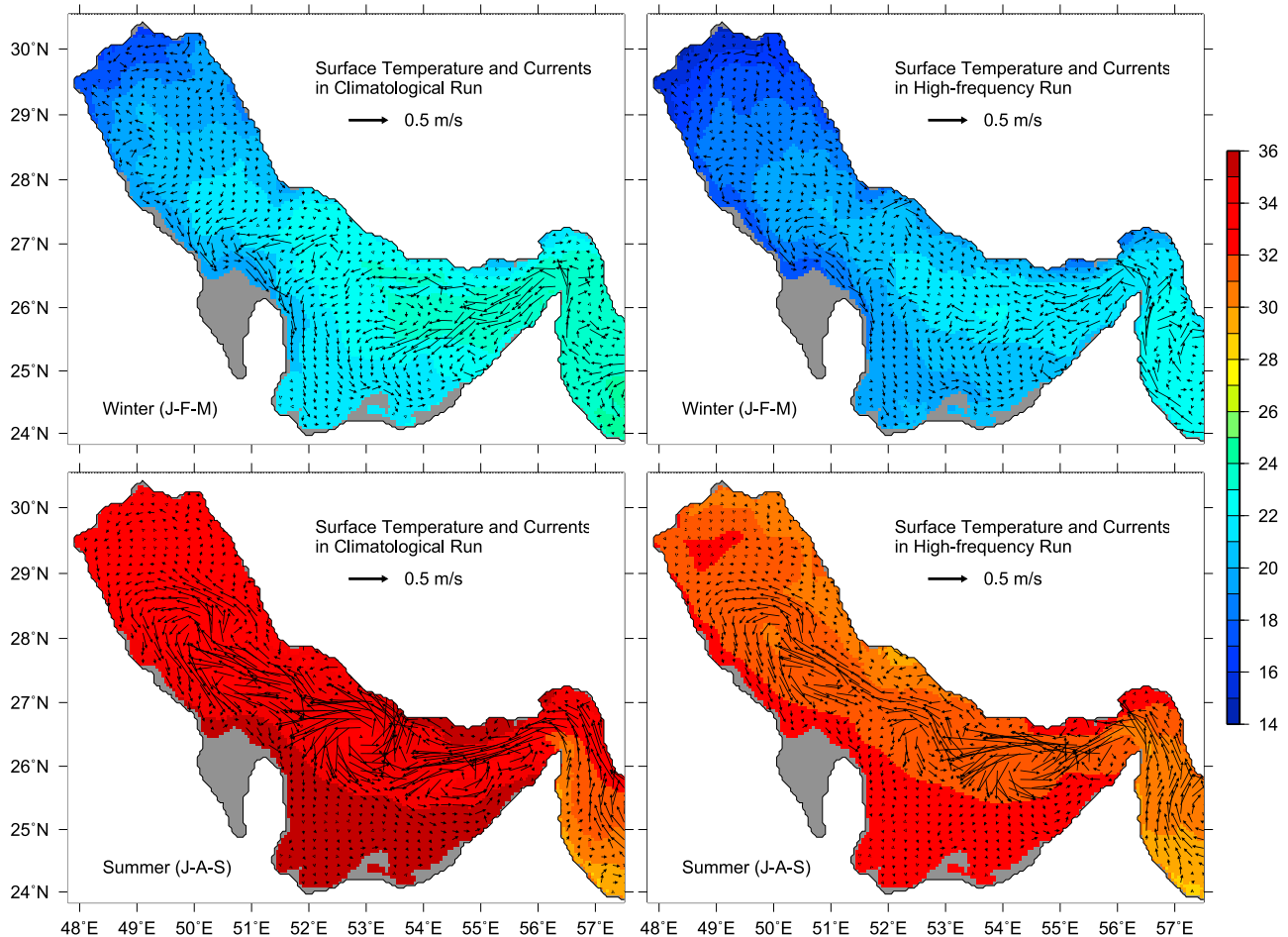


Figure 12. Comparison of the surface temperature fields and currents from high-frequency and climatological run.

where $F_s = -K_V \frac{\partial S}{\partial z} \Big|_{z=0} = S(E - P)$ is the surface salt flux induced by the net evaporation, and $F_b = -K_V \frac{\partial S}{\partial z} \Big|_{z=-h}$ is the salt flux at base of the layer. The equation states that the local variability of the salinity in a fixed water column is determined by the horizontal advection, horizontal diffusion, salt flux at the bottom of the column and the net evaporation at the surface.

[30] The cumulative changes of the mean salinity in the upper 20 m at point P contributed by each term, diagnosed from the 10th year model results in the climatological run, are plotted in Figure 14. The total change resulting from the horizontal advection, surface and vertical mixing flux, and horizontal diffusion agrees to within less than 0.1 psu from the actual salinity change at P in the model, confirming that the diagnosis is accurate. Consistent with the intruding low-salinity IOSW, the effect of the advection in the upper 20 m is generally to lower the surface salinity with an annual cumulative value of -12 psu. The temporary increases in July and September in the advection term are associated with the passing of mesoscale eddies. The vertical mixing flux acts to increase the surface salinity throughout the year with an annual cumulative value of 10 psu. The increase of salinity by the surface evaporation is just about 2 psu over the year. The horizontal mixing contributes little net change over the year, except some disturbances on short time scale. The advection

and vertical mixing flux both have a clear seasonal variability, and it is the interplay between them that essentially controls the change of the surface salinity. From January to March, the two terms almost balance, resulting in rather constant surface salinity. From late March to June, the cumulative effect of vertical mixing flux is small, equivalent to a weak vertical flux of salt, while advection is strong and leads to a decrease of the surface salinity of more than 2 psu. From July to October there are some temporary increases of salinity by advection associated with the two eddies passing over the site in addition to moderate increase in the vertical mixing flux. From November to December, the vertical mixing flux becomes very large, and, despite considerable fresh advection at this time, increases the surface salinity to the winter level.

[31] The change of vertical mixing flux is directly related to the vertical eddy diffusivity (K_V) as seen from the above equation. The vertical distribution of the vertical diffusivity of salt at P is plotted as depth-time contour in Figure 15. A logarithmic scale is used due to the very large variation in K_V . The diffusivity in the surface mixed layer is determined by the surface buoyancy flux and wind stress in the KPP vertical mixing scheme. In response to negative buoyancy flux in winter and fall, the diffusivity is several orders of magnitude larger than in spring and summer. Therefore the change of surface salinity is fundamentally regulated by the seasonal

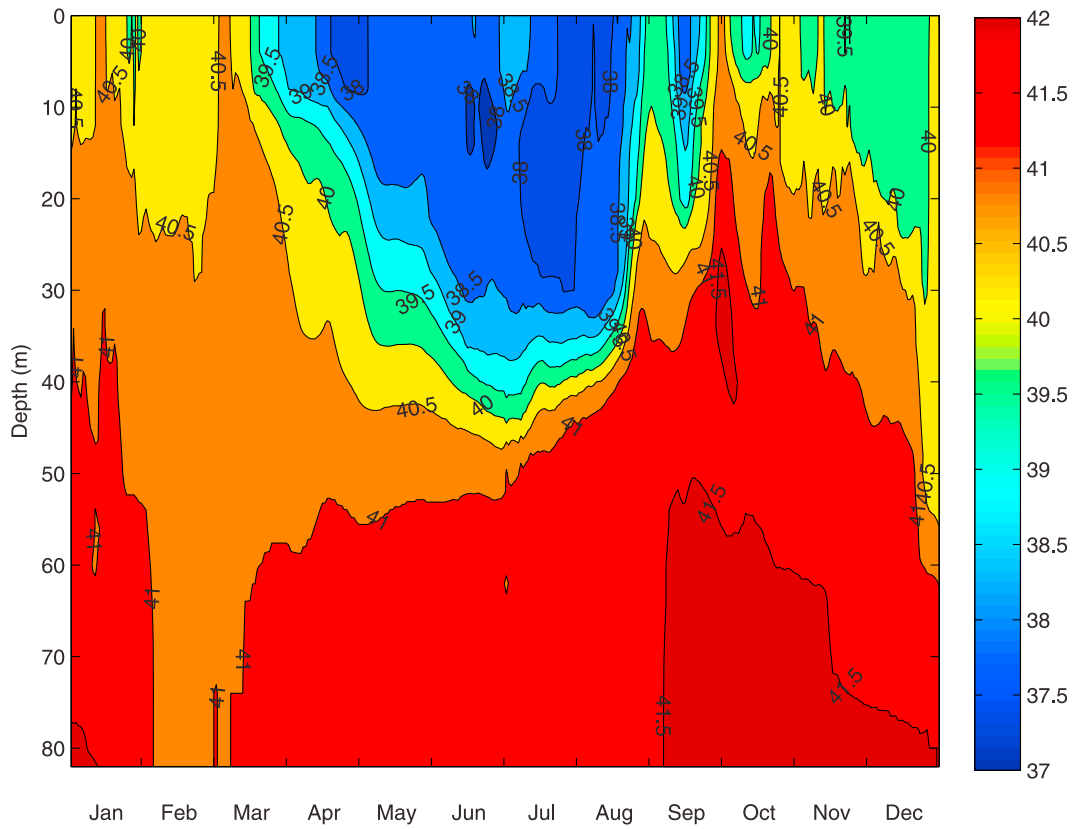


Figure 13. Annual cycle of vertical salinity profiles at the sampling point *P* from the 10th year climatological run. See Figure 5 for location.

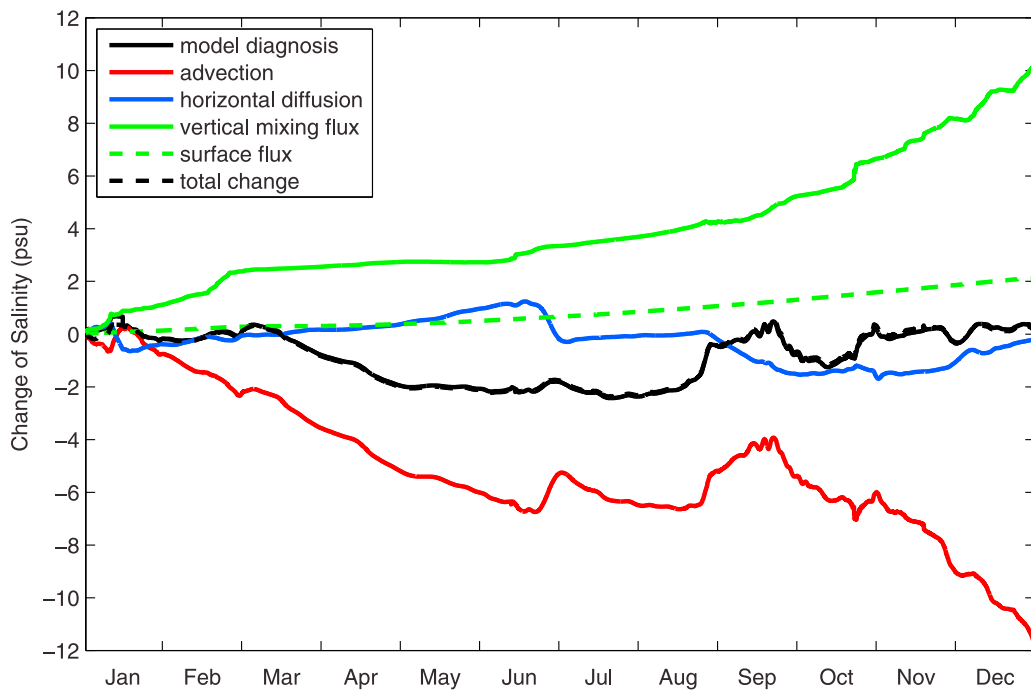


Figure 14. The annual integral change of upper 20 m salinity at the sampling point caused by advection, horizontal diffusion, vertical mixing flux, and surface flux from the 10th year climatological run. Note that the sum of all terms is indistinguishable for the actual seasonal salinity change in the model, confirming that the developed analysis is accurate.

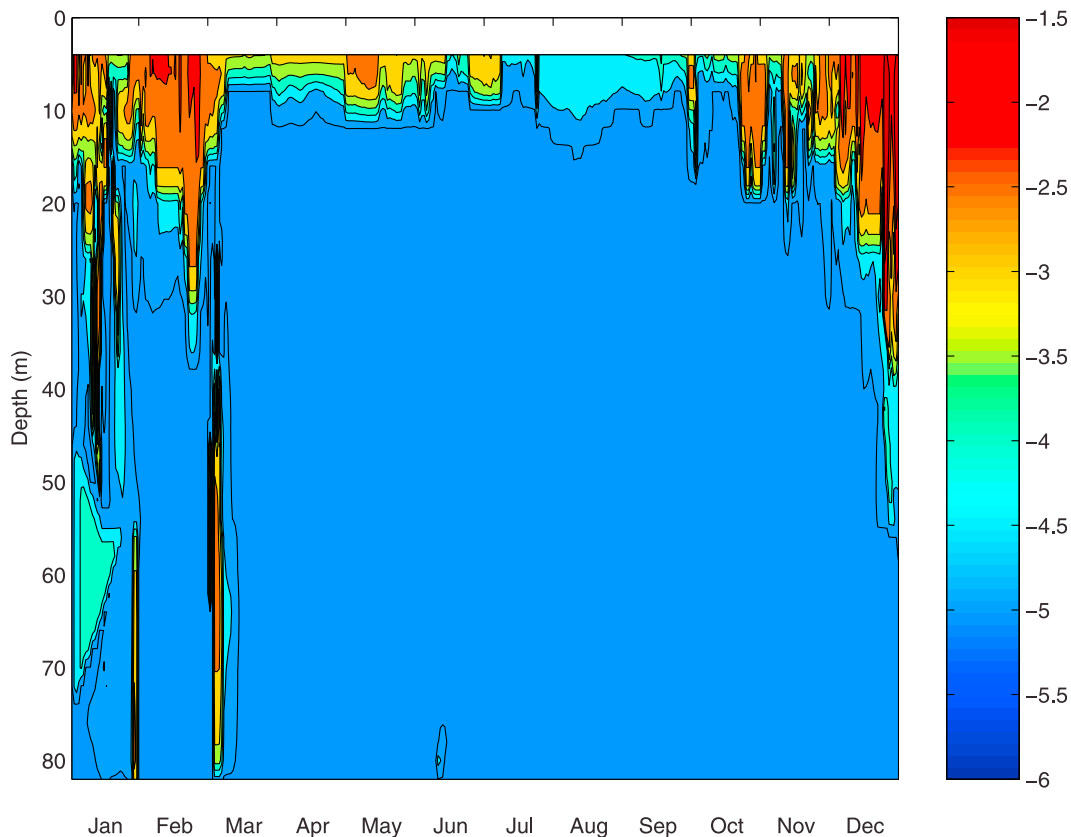


Figure 15. Depth-time contour of the vertical diffusivity of salinity at point P from the 10th year climatological run. The unit of the diffusivity is m^2/s and is plotted on a base 10 logarithmic scale.

heating and cooling cycle, through its influence on the vertical mixing at the base of the mixed layer.

[32] To illustrate these processes over the broader gulf, the spatial distribution of the monthly salinity change in April and December contributed by advection, horizontal diffusion and vertical mixing over the gulf are displayed in Figures 16a and 16b. The monthly contribution caused by the net evaporation is about 0.2 psu over the gulf and is not shown here. In April, the freshening of about 2 psu located between 53° and 54° along the Iranian coast indicates the dominance by advection of the IOSW. The change by vertical mixing and horizontal diffusion are very weak across the basin except in the strait where the mixing is always larger. In December, the salinity change is characterized by an increase located between 54° and 56° and a freshening over the southern banks. Similar to the results found at point P , the main balance over most of the basin at this time is between advection and vertical mixing. In contrast to April, the monthly change in December by vertical mixing is much stronger (~ 3 psu) along the Iranian coast, where it overcomes advection and leads to a salinity increase. The freshening over the coastal southern banks, where depths are less than 20 m and vertical mixing flux is zero here by definition, is caused by advection.

[33] The effect of the seasonal surface wind stress on the surface salinity can be inferred by comparing the surface salinity fields in the climatological run (Figure 10) and those in the buoyancy-only run (Figure 11). Without the northwesterly winds, the IOSW in the buoyancy-only run spreads

considerably farther into the gulf throughout the year, especially in winter. So it can be further stated that the stronger winds in winter play two roles in increasing the surface salinity, first through enhanced vertical mixing, and second through impeding the penetration of IOSW into the basin. Another experiment forced with constant annual mean net evaporation (not shown here) produces a very similar seasonal distribution of the surface salinity to the climatological run and indicates that the seasonal variability of surface evaporation is insignificant in driving the seasonal surface salinity cycle.

7. Summary

[34] The circulation in the gulf is studied using HYCOM with different atmospheric forcing. The surface current fields from the model generally agree with observational features. The surface circulation in the gulf is mainly driven by the low-salinity inflow of IOSW and the surface wind stress. The IOSW propagates in two branches into the gulf: one along the Iranian coast toward the northern gulf, and one veered onto the southern shelf. As suggested by the sensitivity experiment forced only with buoyancy flux, this veering is driven by Ekman drift due to the prevailing northwesterly winds. These branches of inflow form two cyclonic gyres in the northern gulf and in the southern gulf. The surface inflow exhibits significant seasonal variability. The inflow is more intensified along the Iranian coast in summer than in winter,

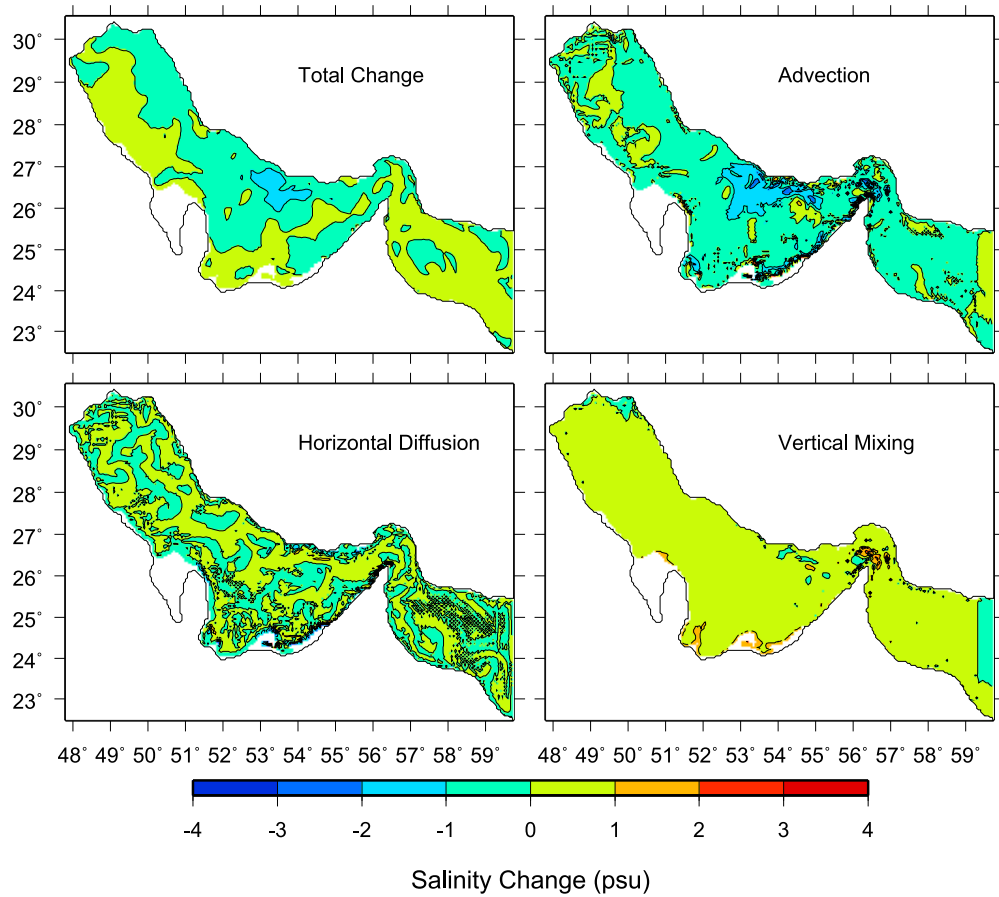


Figure 16a. Monthly change (from the beginning to the end of the month) of surface salinity contributed by individual terms in April, diagnosed from the 10th year climatological run.

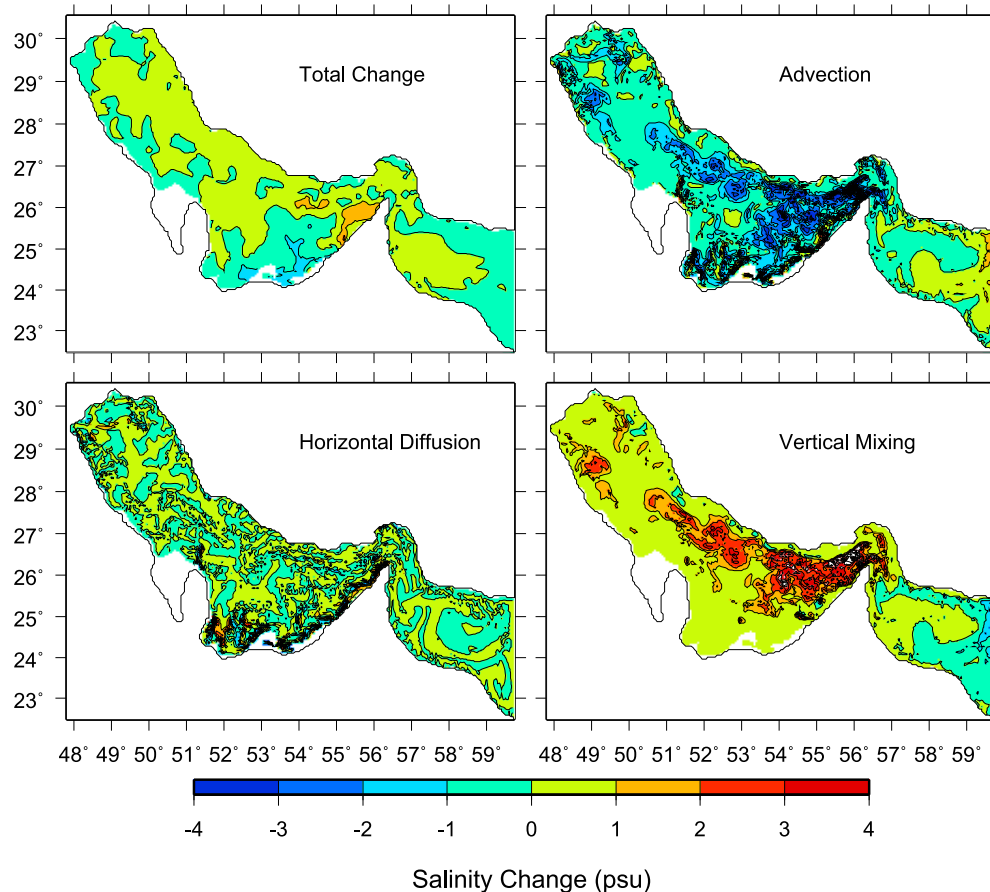


Figure 16b. Same as in Figure 16a but for December.

suggesting more transport of IOSW to the northern gulf. The inflow is shifted more toward the southern gulf in winter due to the stronger northwesterly winds.

[35] One interesting feature of the circulation is the annual cycle of the energetic mesoscale eddies associated with the seasonally migrating salinity front. The eddies develop from the meandering salinity front in spring and form isolated high-salinity cores in summer. The size of the eddies is about 100 km, which is approximately 3 times of the local Rossby deformation radius (~ 30 km). This suggests these eddies are likely the result of a baroclinic instability process, although we have not done an energetics analysis to confirm this rigorously, which is left to further study. The satellite image of surface temperature confirms the existence of the eddies and an unstable front in the gulf.

[36] The surface heat flux and fresh water fluxes parameterized from the high-frequency surface meteorological fields exhibit increased heat and fresh water losses in winter due to the resolved synoptic weather events, and are in better agreement with the fluxes estimated by *Johns et al.* [2003]. The high-frequency atmospheric forcing produces more realistic surface temperatures as a result of the increased heat loss in winter. However the high-frequency forcing does not change significantly the general features of the surface circulation.

[37] The numerical models are successful in reproducing the strong seasonal variation of the surface salinity in the gulf

and provides new insight into the controlling mechanisms. A careful salt budget analysis indicates that it is the balance of the advection of fresh inflow and upward salt flux induced by the vertical mixing that mainly controls the seasonal variation of the salinity in the surface layer. In summer and fall when the vertical mixing is suppressed by the stable thermocline, the IOSW extends farther into the gulf without being greatly modified. In fall and winter, the strong vertical mixing induced by the heat loss leads to upward salt flux that greatly modifies the IOSW, leading to the retreat of the salinity front. Sensitivity experiments suggest that the seasonally varying net freshwater loss ($E - P$) has a little effect in producing this variability. With stronger winds opposing the inflow in winter, the surface wind stress plays a secondary role in modulating in the seasonal variation of the surface salinity. Of the seasonally varying atmospheric forcing including heat fluxes, freshwater flux and wind stress, the heat flux plays the dominant role in producing the seasonal variation of the surface salinity in the gulf through its impact on vertical mixing.

[38] **Acknowledgments.** We would like to thank Alan Wallcraft, George Halliwell, and Eric Chassignet for the invaluable assistance on HYCOM. We also want to thank R. Michael Reynolds for the survey data in the gulf. We are extremely grateful to Wei Zhao and Shuyi Chen for providing the MM5 model output for the gulf region. This work was supported by grant N00014-0310319 from the Office of Naval Research.

References

- Bleck, R. (2002), An oceanic general circulation model framed in hybrid isopycnic-Cartesian coordinates, *Ocean Modell.*, 4(1), 55–88.
- Brewer, P. G., and D. Dyrssen (1985), Chemical oceanography of the Persian Gulf, *Prog. Oceanogr.*, 14, 41–55.
- Canuto, V., A. Howard, Y. Cheng, and M. Dubovikov (2001), Ocean turbulence. Part I: One-point closure model-momentum and heat vertical diffusivities, *J. Phys. Oceanogr.*, 31, 1413–1426.
- Canuto, V., A. Howard, Y. Cheng, and M. Dubovikov (2002), Ocean turbulence. Part II: Vertical diffusivities of momentum, heat, salt, sass, and passive scalars, *J. Phys. Oceanogr.*, 32, 240–264.
- Chandy, J. V., S. L. Coles, and A. I. Abozed (1990), Seasonal cycles of temperature, salinity and water masses of the western Arabian Gulf, *Oceanol. Acta*, 13, 273–281.
- Chao, S. Y., T. W. Kao, and K. R. Al-Hajri (1992), A numerical investigation of circulation in the Arabian Gulf, *J. Geophys. Res.*, 97(C7), 11,219–11,236.
- Csanady, G. T. (1982), *Circulation in the Coastal Ocean*, 279 pp., Kluwer, Boston.
- Dudhia, J. (1993), A nonhydrostatic version of the Penn State-NCAR Mesoscale Model: Validation tests and simulation of an Atlantic cyclone and cold front, *Mon. Weather Rev.*, 121(5), 1493–1513.
- Emery, K. O. (1956), Sediments and water of Persian Gulf, *AAPG Bull.*, 40(10), 2354–2383.
- Halliwel, G. R. (2004), Evaluation of vertical coordinate and vertical mixing algorithms in the Hybrid-Coordinate Ocean Model (HYCOM), *Ocean Modell.*, 7(3–4), 285–322.
- Hunter, J. R. (1982), The physical oceanography of the Arabian Gulf: A review and theoretical interpretation of previous observations, paper presented at 1st Gulf Conference on Environment and Pollution, Kuwait Inst. for Sci. Res., Kuwait City.
- John, V. C., S. L. Cloes, and A. L. Abozed (1990), Seasonal cycles of temperature, salinity and watermass of the Arabian Gulf, *Oceanol. Acta*, 13, 273–81.
- Johns, W. E., F. Yao, D. B. Olson, S. A. Josey, J. P. Grist, and D. A. Smeed (2003), Observations of seasonal exchange through the Straits of Hormuz and the inferred heat and freshwater budgets of the Persian Gulf, *J. Geophys. Res.*, 108(C12), 3391, doi:10.1029/2003JC001881.
- Kämpf, J., and M. Sadrinasab (2006), The circulation of the Persian Gulf: A numerical study, *Ocean Sci.*, 2, 27–41.
- Kara, A. B., P. A. Rochford, and H. E. Hurlburt (2000), Efficient and accurate bulk parameterizations of air-sea fluxes for use in general circulation models, *J. Atmos. Oceanic Technol.*, 17(10), 1421–1438.
- Large, W. G., J. C. McWilliams, and S. C. Doney (1994), Oceanic vertical mixing: A review and a model with a nonlocal boundary layer parameterization, *Rev. Geophys.*, 32, 363–404, doi:10.1029/94RG01872.
- Levitus, S., and T. P. Boyer (1994), *World Ocean Atlas 1994*, vol. 4, *Temperature*, NOAA Atlas NESDIS, vol. 4, 129 pp., NOAA, Silver Spring, Md.
- Levitus, S., R. Burgett, and T. P. Boyer (1994), *World Ocean Atlas 1994*, vol. 3, *Salinity*, NOAA Atlas NESDIS, vol. 3, 111 pp., NOAA, Silver Spring, Md.
- Reynolds, R. M. (1993), Physical oceanography of the Gulf, Strait of Hormuz, and the Gulf of Oman—Results from the *Mt Mitchell* expedition, *Mar. Pollut. Bull.*, 27, 35–59.
- Schott, G. (1908), Der salzgehalt des Persischen Golfes und der angrenzenden gewasser, *Ann. Hydrogr. Mar. Meteorol.*, 36, 296–299.
- Swift, S. A., and A. S. Bower (2003), Formation and circulation of dense water in the Persian/Arabian Gulf, *J. Geophys. Res.*, 108(C1), 3004, doi:10.1029/2002JC001360.
- Thoppil, P. G., and P. J. Hogan (2009), On the mechanisms of episodic salinity outflow events in the Strait of Hormuz, *J. Phys. Oceanogr.*, 39, 1340–1360.
- Woodruff, S. D., S. J. Lubker, K. Wolter, S. J. Worley, and J. D. Elms (1993), Comprehensive Ocean-Atmosphere Data Set (COADS) Release 1a: 1980–92, <http://icoads.noaa.gov/coads1a.html>, Earth Syst. Res. Lab., Boulder, Colo.
- Yao, F., and W. E. Johns (2010), A HYCOM modeling study of the Persian Gulf: 2. Formation and export of Persian Gulf Water, *J. Geophys. Res.*, 115, C11018, doi:10.1029/2009JC005788.

W. E. Johns and F. Yao, Division of Meteorology and Physical Oceanography, Rosenstiel School of Marine and Atmospheric Science, University of Miami, 4600 Rickenbacker Cswy., Miami, FL 33149, USA. (bjohns@rsmas.miami.edu; fyao@rsmas.miami.edu)